Microwave Studies of the Electron Loss Processes in Gaseous Discharges*

ROMAYNE F. WHITMER†
Los Alamos Scientific Laboratory, Los Alamos, New Mexico
(Received June 13, 1956)

A method for studying electron loss processes in gaseous discharges by means of the free transmission of microwave signals through the discharge is discussed. This method has the advantage that it is easily adaptable to any size or shape of discharge tube. The electron loss processes in pure hydrogen have been studied using this method. For electron densities of 5×10^{13} cm^{-3}, the electron-ion recombination coefficient has been found to be approximately 5.9×10^{-11} cm^{-3} sec^{-1}. An electron-neutral collision frequency of 3.97×10^{9} sec^{-1} at a pressure of 0.29 mm Hg has been measured. The dominant loss process proved to be attachment, with a probability of attachment of approximately 3×10^{-6}.

INTRODUCTION

MICROWAVE techniques have been used for some time in the study of electron loss processes in the afterglow of gaseous discharges.[1–3] The method generally used is to measure the change in the resonant frequency of a cavity containing the discharge, thus measuring the electron density. Such a method has the disadvantage that the discharge tube must be constructed to suit the microwave equipment; however, it might not be feasible to adapt a given discharge tube to the cavity-type arrangement. A method will be described which can be used on most discharge tubes and also allows the use of other than microwave equipment to monitor the discharge.

Little agreement had been reached as to the loss processes in hydrogen until Persson and Brown[4] clearly pointed out the importance of impurities in these processes. They were able to give a precise measurement of the ambipolar diffusion coefficient in hydrogen but could not determine the recombination coefficient. The main limitation on the measurement of the recombination coefficient is the maximum electron density that it is possible to measure. Since the method to be described does not involve cavity-type structures, it was possible to use millimeter waves and measure electron densities of 5×10^{13} cm^{-3}. This permitted the measurement of the recombination coefficient and attachment losses but it was not possible to detect ambipolar diffusion losses.

THEORY

For plane wave propagation through an ionized gas, it can be shown[5] that γ, the propagation constant of the wave, is related to the electron density by

$$\gamma^2=-\mu_0\epsilon_0\omega^2\epsilon', \tag{1}$$

where

$$\epsilon'=1+\frac{\sigma_r}{j\omega\epsilon_0}+\frac{\sigma_i}{\omega\epsilon_0}, \tag{2}$$

$$\sigma_r=\frac{Ne^2}{m\omega}\frac{\nu/\omega}{1+(\nu/\omega)^2}, \tag{3}$$

and

$$\sigma_i=-\frac{Ne^2}{m\omega}\frac{1}{1+(\nu/\omega)^2}, \tag{4}$$

in the absence of any external magnetic fields. Mks units are used throughout. N=number of electrons per cubic meter, ϵ_0=dielectric constant of free space, e=charge of electron, m=mass of electron, μ_0=permeability of free space, ν=collision frequency of electrons with neutral particles, ω=transmitted signal frequency, and $\sigma=\sigma_r+j\sigma_i$=conductivity of media. It is assumed that ν is not dependent on the velocity of the electrons. For the case $(\nu/\omega)^2\ll1$, Eqs. (3) and (4) reduce to

$$\sigma_r=(Ne^2/m\omega)(\nu/\omega) \tag{5}$$

and

$$\sigma_i=-(Ne^2/m\omega), \tag{6}$$

and Eq. (2) becomes

$$\epsilon'=1-(\omega_p/\omega)^2-j(\omega_p/\omega)^2(\nu/\omega), \tag{7}$$

where ω_p, the plasma frequency, is given by

$$\omega_p=(Ne^2/m\epsilon_0)^{\frac{1}{2}}. \tag{8}$$

By setting

$$\gamma=\alpha+j\beta, \tag{9}$$

and substituting Eq. (7) into Eq. (1), one obtains

$$\frac{\alpha}{\omega}\cong\frac{1}{2c}\left(\frac{(\omega_p/\omega)^2\nu/\omega}{[1-(\omega_p/\omega)^2]^{\frac{1}{2}}}\right) \tag{10}$$

and

$$\beta/\omega\cong(1/c)[1-(\omega_p/\omega)^2]^{\frac{1}{2}}, \tag{11}$$

where α is the attenuation factor and β is the phase constant. It can be seen that a measurement of the change in the phase of a wave transmitted through an ionized gas with respect to a reference path will yield N.

* Work done under the auspices of the U. S. Atomic Energy Commission.
† Sylvania Electric Products, Inc., Mountain View, California.
[1] M. A. Biondi and S. C. Brown, Phys. Rev. **75**, 1700 (1949).
[2] L. J. Varnerin, Phys. Rev. **84**, 563 (1951).
[3] J. M. Anderson and L. Goldstein, Phys. Rev. **100**, 1037 (1955).
[4] K. B. Persson and S. C. Brown, Phys. Rev. **100**, 729 (1955).
[5] H. Margenau, Phys. Rev. **69**, 508 (1946).

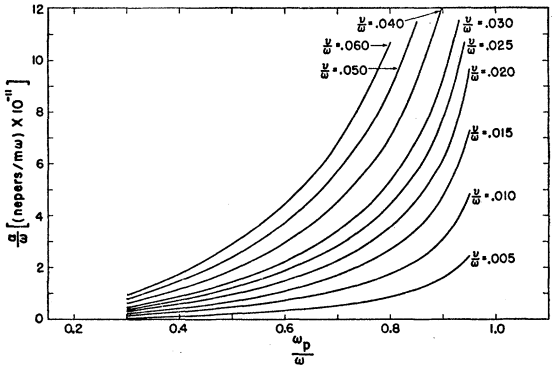

FIG. 1. Signal attenuation *versus* density for various values of ν.

By similarly measuring the attenuation, ν may be obtained. The function described in Eq. (10) is plotted in Fig. 1.

THE MICROWAVE INTERFEROMETER

The arrangement of the microwave components into an interferometer is shown in Fig. 2. The detected output of the crystal, which is operated in the linear region, can be shown to be:

$$\text{detected output}=[A^2+B^2+2AB\cos(\beta-\beta_0)z_g]^{\frac{1}{2}}, \quad (12)$$

where A is the amplitude and β is the phase constant of the signal passing through the reference path. The phase shifter in the reference path was adjusted such that when $N=0$, that is $\beta=\beta_0$, the waves through the two paths were 180 degrees out of phase. Usually B would be adjusted, by means of the attenuator in the reference path, to give a perfect null in the absence of the ionized gas. However it was found that much better sensitivity was obtained by using the null path signal to provide rf bias for the crystal. For this case $B\gg A$ and therefore

$$\text{detected output}\cong B+A\cos(\beta-\beta_0)z_g. \quad (13)$$

It has proven more convenient to identify the output with electron density only at the maximum and minimum values of the function described by Eq. (13). For these values,

$$N=\frac{m\epsilon_0\pi cn}{e^2z_g}\left(\frac{n\pi c}{z_g}+2\omega\right), \quad (14)$$

where $n=1, 3, 5, 7, 9, \cdots k$. This treatment assumes N to be uniform throughout the volume of the gas encompassed by the microwave horns. Since the electron density that is measured is an average density over this volume, it is believed that this assumption does not introduce an appreciable error in the measurement. The function described in Eq. (14) is plotted in Fig. 3 for one value of z_g.

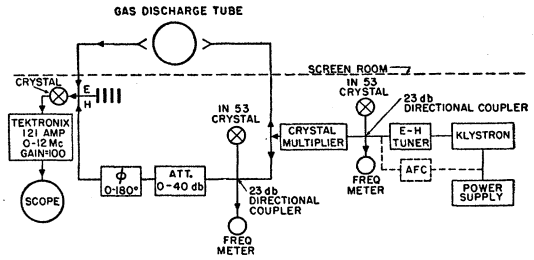

FIG. 2. The microwave interferometer.

THE DISCHARGE SYSTEM

A simplified diagram of the experimental arrangement is shown in Fig. 4. The discharge tube consisted of two Pyrex cylinders one mounted on top of the other. The large cylinder was $9\frac{5}{8}$ inches in diameter and 8 inches high. The smaller cylinder was $3\frac{3}{8}$ inches in diameter and 4 inches high. A torus of $\frac{1}{2}$-inch diameter Pyrex tubing was mounted on top of the upper cylinder. The high-vacuum system consisted of an oil-fractionating glass pump trapped with liquid nitrogen. The discharge system was baked for 18 hours at 460°C before each set of data was taken. A vacuum of 5×10^{-8} mm Hg could be maintained. Hydrogen could be let into the system at controlled pressures by heating uranium hydride, contained in a quartz tube, to about 200°C. The hydrogen pressure was measured by means of a Autovac vacuum gauge which had been calibrated for hydrogen against a McLeod gauge.

Energy was coupled into the gas inductively by means of a transformer core which linked the torus. A condenser bank was charged to 20 kv and discharged through the one-turn primary winding on the transformer core. A field of approximately 1000 v cm^{-1} around the torus was obtained in this manner. When the gas in the torus ionized, it formed a shorted secondary of the transformer. It was necessary to put a 0.1-ohm resistor in the primary circuit and a 10-mil gap in the transformer to reduce ringing. A pulse of 5-μsec duration was obtained with a negative pulse of 10% amplitude following approximately 10 μsec later.

The microwave horns were placed at eight different positions on the large cylinder. These included two vertical positions on the cylinder as well as different positions around the cylinder. Also one set of data was taken with the horns offset from the diameter of the cylinder. All positions gave essentially the same results as far as the quantities measured are concerned.

The scope was triggered by means of a pulse from a pickup loop linking the transformer core.

EXPERIMENTAL RESULTS

The first measurements made were with a 1.5-meter Wadsworth spectrograph, which had an effective stop of $f/20$, in an attempt to determine the purity of the discharge. At a point approximately 1 cm below the

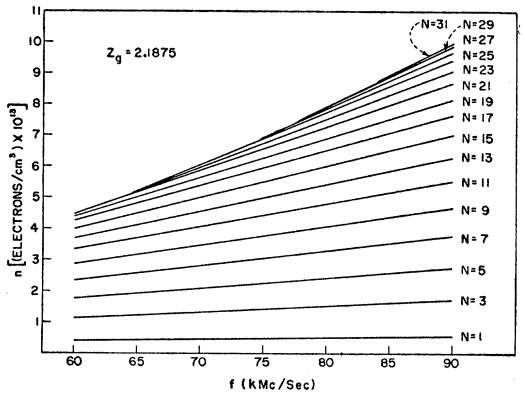

FIG. 3. Electron density *versus* frequency for values of n.

entrance of the torus to the upper cylinder the following, and only the following, lines were observed: H_α, H_β, H_γ, B^+, B^{++}, Si^+, Si^{++}, and Si^{+++}. At a position in the middle of the large cylinder only H_α, H_β, and H_γ lines were observed. It is apparent that the B and Si ions were produced by very fast electrons striking the wall of the torus. These electrons boil off the ions and eventually these ions were injected into the upper cylinder. However, the absence of these lines in the large cylinder is not conclusive evidence of the purity in that portion of the tube. In order to observe the hydrogen lines it was necessary to expose the spectrograph to one hundred discharges. This may not have been sufficient to detect the impurities.

Figure 5 shows the results of the attenuation measurements. This attenuation appears superimposed on the detected output of the crystal as given by Eq. (13) and yields the collision frequency ν after applying the curves of Fig. 1. The relation between ν and the pressure p is

$$\nu = 1.73\times10^9 p + 3.47\times10^9, \qquad (15)$$

where p is in mm Hg. This gives a value for ν which is not as dependent on p as has previously been reported[6]; however, it is not felt that this is significant. In Fig. 6 is plotted the natural logarithm of the electron density as a function of time, indicating the linearity of this plot for large values of time or lower densities. In Fig. 7

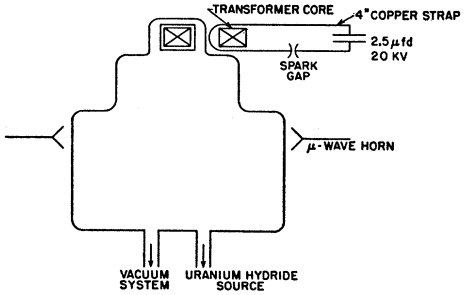

FIG. 4. The discharge system.

[6] R. B. Brode, Revs. Modern Phys. **5**, 256 (1933).

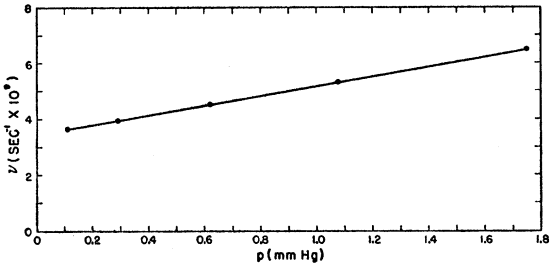

FIG. 5. Plot of the collision frequency *versus* pressure.

is plotted the reciprocal of the electron density as a function of time, indicating the linearity of this plot at high densities. It should be noted that the time $t=0$ is actually 150 to 200 μsec after the gas was ionized.

ANALYSIS OF THE RESULTS

The basic loss processes in the afterflow can be described by

$$\partial n/\partial t = D_a\nabla^2 n - h\nu n - \alpha n^2, \qquad (16)$$

where n is the electron density in cm^{-3}, D_a is the ambipolar diffusion coefficient, h is the probability of an electron attaching to a neutral particle forming a negative ion, and α is the electron-ion recombination coefficient. It is assumed that the number of electrons equals the number of positive ions and that the electrons and ions are in thermal equilibrium with the gas molecules. If one momentarily assumes that the dominant loss is due to diffusion, Eq. (16) can be written as

$$\partial n/\partial t = (D_a/\Lambda^2)n - h\nu n - \alpha n^2, \qquad (17)$$

where Λ is the characteristic diffusion length of the large Pyrex cylinder. For this geometry $\Lambda^2 = 6.35$ cm, and for the above assumption D_a/Λ^2 equals the slopes of the linear portions of the curves plotted in Fig. 6. Therefore a value of $D_a = 1.28\times10^5$ would be calculated from the curve of $p=0.29$ mm Hg. This is in obvious disagreement with the value of $D_a = (700\pm50)p$ given by Persson and Brown.[4]

Assuming, therefore, that diffusion can be neglected Eq. (16) becomes

$$\partial n/\partial t = -h\nu n - \alpha n^2, \qquad (18)$$

and for the lower values of n attachment is the dominant loss process. Since ν has been previously evaluated, the

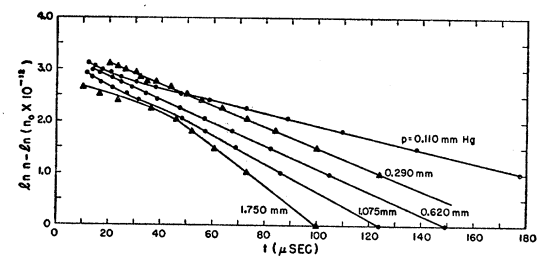

FIG. 6. The electron decay in the late afterglow.

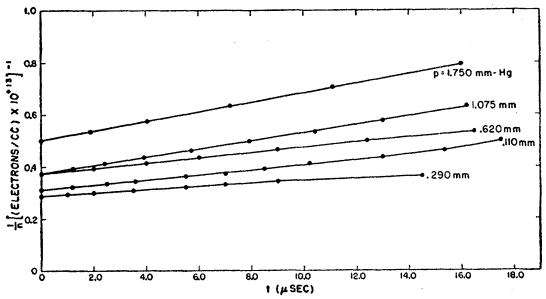

FIG. 7. The electron decay in the early afterglow.

slopes of the curves of Fig. 6 yield h. These results are given in Table I. The solution to Eq. (18) can be written as

$$\frac{1}{n}=\frac{1}{n_0}e^{h\nu t}+\frac{\alpha}{h\nu}(e^{h\nu t}-1), \tag{19}$$

where $n=n_0$ when $t=0$. The slope of Eq. (19) can be written as

$$\frac{d}{dt}\left(\frac{1}{n}\right)=\left(\frac{h\nu}{n_0}+\alpha\right)(1+h\nu t) \tag{20}$$

to the first order in t. For t such that $h\nu t\ll 1$, this slope, called α', is given by

$$\alpha'=(h\nu/n_0)+\alpha. \tag{21}$$

This explains why the curves of Fig. 7 are straight lines. When α' is determined from the curves, α can be calculated and is tabulated in Table I.

The quantities on the right-hand side of Eq. (17) can now be compared as to orders of magnitude. This gives, for $p=0.29$ mm Hg,

$$\begin{aligned}\text{diffusion}&—(D_a/\Lambda^2)n\cong 7\times 10^{15},\\ \text{attachment}&— h\nu n \cong 6\times 10^{17},\\ \text{recombination}&— \alpha n^2 \cong 5.4\times 10^{16},\end{aligned}$$

which is in agreement with the assumptions. It can be seen that the recombination term only has an effect at the higher densities. It is felt that the value $\alpha=5.9\times 10^{-11}$ cm^{-3} sec^{-1} is the best value since it was measured at the highest density.

One possible source of error in the measurement of the electron density could be caused by reflections of the microwave signal off of the ionized gas. These could cause false interferometer patterns. The reflected signal was monitored and found to be completely negligible except during the time in which $\omega_p>\omega$, as would be expected. Even during this time the reflected signal was a factor 10 down in amplitude as compared with the transmitted signal when $\omega_p<\omega$.

CONCLUSIONS

Very little comparison of these results with that of other workers is possible since the electron densities studied here are approximately a factor of 10^3 higher than has previously been reported. The collision frequency agrees with that given by Brode[6] if it is assumed that the electron energy is four electron volts. From the spectroscopic studies it appears likely that the electron energy was at least one electron volt. The recombination coefficient is in closer agreement with the theoretical value than other workers have reported. The difference between the theoretical and experimental values is probably explained by the impurities. Professor S. C. Brown of the Massachusetts Institute of Technology has suggested that the high recombination coefficient which he and his co-workers measured originally was actually the attachment coefficient measured here. He reasons that this attachment is due to the presence of water vapor in the discharge tube.

TABLE I. Summary of the data.

p(mm Hg)	ν(sec^{-1})	h	α(cm^{-3} sec^{-1})
0.110	3.67×10^9	3.19×10^{-6}	5.15×10^{-10}
0.290	3.97×10^9	5.06×10^{-6}	5.9×10^{-11}
0.620	4.51×10^9	4.76×10^{-6}	9.2×10^{-11}
1.075	5.35×10^9	5.20×10^{-6}	5.50×10^{-10}
1.750	6.50×10^9	5.86×10^{-6}	4.2×10^{-11}

If the transmitted signal frequency could be increased by a factor of two, electron densities of 1.5×10^{14} cm^{-3} could be measured and recombination would be the dominant loss process in the early afterglow. This would greatly enhance the accuracy of the measurement of α, however, the availability of microwave power at this frequency excludes this possibility at this time.

Owing to the lack of information as to the electron energy, it is not felt that cross-section evaluations from h and ν are meaningful.

ACKNOWLEDGMENTS

The author wishes to thank Dr. F. R. Scott for the spectroscopic measurements and Mr. R. B. Ferrell for the construction and operation of the discharge system. The loan of a millimeter wave wafer-type crystal and detector mount from Mr. W. Sharpless of Bell Telephone Laboratories greatly increased the sensitivity of the system.